LA-UR -81-1421

TITLE: LAGRANGIAN FLUID DYNAMICS USING THE VORONOI-DELAUNAY MESH

MASTER

AUTHOR(S): John K. Dukowicz

SUBMITTED TO: To be presented at the International Conference on Numerical Methods for Coupled Problems, Sept. 1981, Swansea, United Kingdom

University of California

LOS ALAMOS SCIENTIFIC LABORATORY
Post Office Box 1663 Los Alamos, New Mexico 87545
An Affirmative Action/Equal Opportunity Employer

Form No. 836 R3
St. No. 2629
12/73

UNITED STATES
DEPARTMENT OF ENERGY
CONTRACT W 7405 ENG. 36

LAGRANGIAN FLUID DYNAMICS

USING THE VORONOI-DELAUNAY MESH

John K. Dukowicz

Theoretical Division, Group T-3
Los Alamos National Laboratory
University of California
Los Alamos, NM 87545

ABSTRACT

A Lagrangian technique for numerical fluid dynamics is described. This technique makes use of the Voronoi mesh to efficiently locate new neighbors, and it uses the dual (Delaunay) triangulation to define computational cells. This removes all topological restrictions and facilitates the solution of problems containing interfaces and multiple materials. To improve computational accuracy a mesh smoothing procedure is employed.

I. INTRODUCTION

There are two general classes of methods for the numerical solution of fluid dynamics problems. This classification is determined by whether Eulerian coordinates are used, in which a prescribed, fixed mesh is employed, or whether Lagrangian coordinates are used, in which the mesh is embedded in the fluid and is carried along with it. The Eulerian approach is the most common. The Lagrangian method has several distinct advantages, but the difficulties of implementing such a method, except in the one-dimensional case, have not made it equally popular.

In the Lagrangian formulation the conservation equations take their simplest form. In particular, the nonlinear convection terms which often cause a great deal of inaccuracy associated with "numerical smearing", are absent. Since the mesh travels with the flow, an initially adequate zoning will generally remain adequate. Certain features of fluid flows, such as free surfaces and interfaces between dissimilar materials, travel with the flow and are therefore particularly well resolved by Lagrangian methods.

The two main problems with Lagrangian methods are mesh tangling and numerical inaccuracy due to highly irregular meshes. The first problem, that of mesh tangling, has received the most attention. The problem arises because a mesh of fixed topology quickly becomes singular in flows undergoing large distortions. There are two solutions: rezoning and reconnection. In rezoning, the distorted mesh is mapped onto a more regular mesh. In reconnection, the mesh topology is changed such that mesh points acquire new neighbors. Methods which thus circumvent topology restrictions are commonly called free Lagrangian methods. It should be noted that both of these methods of reconstructing the mesh involve reapportionment of mass, momentum, and energy among the mesh cells

affected, and this represents a reappearance, to some extent, of the undesired convective fluxing characteristic of Eulerian methods.

The second issue is less commonly addressed. Even with a satisfactory mesh topology, containing suitably convex cells, the evolution of the flow may produce a highly distorted, uneven mesh that is unsuitable for accurate approximation.

One of the most successful Lagrangian techniques is the PIC method[1]. However, this cannot be considered a representative Lagrangian method, in the sense of this paper, since there is no moving mesh. It is, rather, a prominent example of the particle methods. In the PIC method, the flow is represented by large numbers of particles carrying mass, momentum, and energy. The particles are accelerated by a pressure gradient determined by counting particles in a fixed, relatively coarse mesh. Other particle schemes[2-4] are more closely related in spirit to molecular dynamics calculations. An interparticle force is specified, which is usually related to the equation of state. Harlow[5] has shown that the PAF (particle-and-force) method[4] is equivalent to solving the equations of fluid dynamics in a statistical sense. That this is true for all such particle methods might be expected from statistical mechanics considerations. However, for the relatively small number of particles that can be realistically used, the statistical fluctuations are large and therefore it is to be expected that solving the mean equations using an equivalent number of mesh points would be more profitable.

A strictly Lagrangian numerical method is restricted to those limited cases in which mesh tangling does not occur, as in one-dimensional geometries, or in situations made effectively one dimensional due to symmetry, or for limited evolution times. To overcome mesh tangling problems, the most common approach is exemplified by the ALE technique[6]. In this technique, a mesh of

quadrilateral cells is applied in several phases. In essence, there is first a Lagrangian phase, followed by a rezone phase in which mesh points are moved to prescribed positions. The rezone may occur at every time step, in which case it is termed a continuous rezone, or it may occur after many time steps but before the mesh is in danger of tangling, in which case some form of interpolation is employed to transfer variables from one mesh to the other. The rezoned mesh most frequently preserves the topology of the original mesh, and in fact it is often just the regular mesh formed by the intersection of perpendicular straight lines.

An alternative to this type of rezoning is provided by the free Lagrangian methods[7,8]. In these methods, the topology is changed by choosing new neighbors based on some suitable criterion. In order to be free of topological constraints, the resulting meshes are triangulations in two dimensions. The criterion for locating neighbors may be based on the distance between points (nearest neighbors), or on some measure of the vertex angles of the triangulation. The resulting mesh is usually found by iteration[7,8], or else it might be obtained by some variation of the bin sorting algorithm for finding nearest neighbors[4,9]. Other approaches, not described in the literature, are possible and are being pursued. It may be said, however, that while these techniques overcome the problems of mesh tangling they do not solve the problem of mesh irregularity.

In the present paper we will describe a technique which addresses both of these issues. This technique combines the advantages of the free Lagrangian methods with their unrestricted topology, with the improved numerical accuracy made possible by selective continuous rezoning. A particularly efficient method for changing mesh topology is used which is based on the construction of the Voronoi mesh, which will be defined and fully described later. The problem of

mesh irregularity is overcome by allowing the mesh to slip with respect to the flow in order to set up an essentially regular local mesh. The mesh is maintained strictly Lagrangian in those parts of the flow where this is required, such as at interfaces. This slippage introduces convective fluxing, but on the other hand the mesh regularization greatly reduces mesh reconnection and its associated fluxing. It should be stressed that this fluxing is not nearly as severe as that in Eulerian calculations since the mesh still moves with approximately the local flow velocity.

This method will be described in one of its simplest possible implementations. That is, it will be limited to two-dimensional Cartesian coordinates and inviscid, compressible flow with an equation of state in which the pressure is a function of the density only. Simple examples are the isentropic and the Chaplygin equations of state. Such an implementation will illustrate all the main features of the method in a realistic context, without unnecessary complications. It is anticipated that there is nothing that would prevent the extension of the techniques described to more generally interesting situations involving an energy equation, viscosity, multiple materials, cylindrical coordinate systems, or three dimensions.

II. THE VORONOI MESH

Free Lagrangian techniques are characterized by mesh points changing their neighbors during a calculation. There is a variety of techniques for locating new neighbors[7-9]. The Voronoi mesh is a geometrical construction associated with a random distribution of points in space[10,11] that appears to be uniquely well suited to this application.

The Voronoi mesh may be defined as the subdivision of space, associated with a random set of points, into a set of convex polygons (polyhedra in 3-D) such that all space inside a polygon is closer to the enclosed point than to any other point. The faces of the polygons are segments of the perpendicular bisectors of the lines joining neighboring points. A small fragment of a Voronoi mesh is illustrated in Fig. 1. (We limit the discussion here to two dimensions but the Voronoi mesh is defined in a space of arbitrary dimensionality[10,11]). The Voronoi construction is not widely known but it has found applications in solid state[12] and liquid state[13] theory, astrophysics[14], microemulsions[15], rock structure[16], and theories of computational complexity[17].

The Voronoi mesh possesses a number of properties, some of which are especially important in our application. Associated with the Voronoi mesh is a dual mesh, formed by joining the neighboring points, which is called the Delaunay triangulation[10,18]. This dual mesh is indicated by dashed lines in Fig. 1. The vertices of the Voronoi polygons are called the Voronoi points. The Voronoi points are the circumcenters of the Delaunay triangles (centers of the circles circumscribing the triangles). Each line joining neighbors is the diagonal of a quadrilateral formed by two adjoining triangles. This diagonal divides that pair of opposite angles of the quadrilateral that sum to more than 180°. Contrary to the assertion of Shamos and Hoey[17], the Delaunay triangulation does not have the minimum total side length.

The most important property of the Voronoi mesh is that it is unique and continuous. That is, a continuous translation of the points (centers) defining the Voronoi mesh produces a continuous change in the Voronoi mesh. This process is illustrated in Fig. 2. As neighbors change, the associated polygon side length decreases to zero and then a new side begins to form associated with the new neighbors. When the side length goes to zero, two Voronoi points merge and all four associated centers are located on the circumference of a single circle. This shows us that a known pair of neighbors is always formed whenever another pair of points is separated, and vice-versa. This, therefore, obviates the need to search for nearest neighbors.

The property of continuity assures us that we can follow the evolution of the Voronoi mesh in this simple manner provided the time step is sufficiently short. A sufficient condition for this is that a point stay within its already defined Voronoi polygon during a time step. This implies that we must start from an existing Voronoi mesh at the initial time. We are thus faced with the task of constructing an initial Voronoi mesh.

There exist published algorithms for constructing arbitrary Voronoi meshes in three dimensions[19,20]. Shamos and Hoey[17] suggest an ingenious algorithm for two dimensions. For our purposes it is sufficient to start from a regular rectangular or hexagonal arrangement of points for which the Voronoi mesh is obvious.

The actual algorithm for finding new neighbors consists of a single pass through the mesh "disconnecting" the appropriate diagonal, and at the same time "connecting" the corresponding diagonal according to which pair of opposite angles of a quadrilateral sums to more than 180°. The continuity property ensures that all such connections will be properly considered in a single pass, and it is easy to ensure that redundant checking does not take place. It is of

interest to note that the average number neighbors in the Delaunay triangulation, as in any planar triangulation. is six, whenever the number of boundary points is small compared to the total number of points.

III. EQUATIONS AND DIFFERENCING

The prototypic equations which we will consider are the equations of inviscid, compressible gas dynamics given by

$$\frac{\partial}{\partial t}\rho + \underline{\nabla}\cdot\rho\underline{u} = 0, \tag{1}$$

$$\frac{\partial}{\partial t}\rho\underline{u} + \underline{\nabla}\cdot\rho\underline{u}\underline{u} = -\underline{\nabla} p, \tag{2}$$

together with the special equation of state

$$p = p(\rho) \ . \tag{3}$$

This equation of state uncouples and eliminates the energy equation, and thus simplifies the system. Examples are the isentropic equation of state ($p = p_\infty(\rho/\rho_\infty)^\gamma$, and the Chaplygin equation of state ($p = k^2(1/\rho_\infty - 1/\rho)$).

It is frequently desirable, especially for compressible flow, to formulate difference equations which preserve the conservation property of the differential equations. This is most easily done by writing the equations in the control volume form[21]

$$\frac{d}{dt}\int_V \rho dV + \int_S \rho(\underline{u}-\underline{b})\cdot\underline{n}dS = 0 \ , \tag{4}$$

and

$$\frac{d}{dt}\int_V \rho\underline{u}dV + \int_S \rho\underline{u}(\underline{u}-\underline{b})\cdot\underline{n}dS = -\int_S p\underline{n}dS, \tag{5}$$

where V(t), S(t) are the time varying volume and surface of the control volume, $\underline{n}$ is the unit vector, normal to the surface, pointing outwards, and $\underline{b}$ is the surface velocity. The surface integrals involving the surface velocity $\underline{b}$ are the convective fluxing terms. We can define

$$m = \int_V \rho dV \tag{6}$$

to be the control volume mass and

$$\hat{\underline{u}} = \frac{1}{m} \int_V \rho \underline{u} dV \tag{7}$$

to be the mean control volume velocity. This defines the control volume position through

$$\frac{d}{dt}\hat{\underline{x}} = \hat{\underline{u}} \ . \tag{8}$$

In the special case of $\underline{b} = \underline{u}$ there is no fluxing across the control surface and the control volumes are Lagrangian, i.e.

$$\frac{dm}{dt} = 0, \tag{9}$$

and

$$m \frac{d}{dt}\hat{\underline{u}} = -\int_S p\underline{n} ds. \tag{10}$$

Equation (6) could be used to define a mean density

$$\hat{\rho} = \frac{\int_V \rho dV}{V} = \frac{m}{V} \tag{11}$$

where $V = \int_V dV$ is the cell volume, and this gives the pressure from the equation of state $p = p(\hat{\rho})$.

The choice of control volume is somewhat arbitrary. At first sight the use of the Voronoi polygon as the control volume appears natural[22]. However, there are several reasons why this is not attractive. The straightforward evaluation of the term involving the integral of surface pressure, using the average of neighbor cell pressures, is not consistent with the differential equations since this pressure is not centered along the cell face. To overcome this, it is necessary to evaluate the Voronoi point coordinates, and to interpolate among local pressures to find the pressure at the cell vertices. This adds a considerable amount f computation. Further, the cell vertices are determined strictly from geometrical considerations and therefore do not travel with the

local flow velocity. This means that the cells are not Lagrangian (the cell points are), and fluxing across cell faces is necessary. In addition, the cell points are not centered within their cells and as we shall see later, this leads to numerical inaccuracy.

An alternative choice is the control volume formed by all the triangles of the Delaunay mesh surrounding a cell point, as illustrated in Fig. 3a. There is triple overlap of these cells, so that the actual volume of a cell is equal to a third of the total volume of its triangles. This control volume appears to be most applicable to those variables that are defined at the cell points (or triangle vertices). Another choice is the cell formed by joining triangle centroids and the mid-points of triangle sides[23], as illustrated in Fig. 3b. This cell appears to be appropriate to those variables which are defined on the triangles. The volumes of these two types of cells are equal.

Both of these cells are Lagrangian in the sense that all vertices of the cell move with local flow velocity ($\underline{b} = \underline{u}$), so that no fluxing is required. The volume (area) of the cells is

$$V_j = \frac{1}{6} \underline{Z} \cdot \sum_i (\underline{r}_{i-1} \times \underline{r}_i), \tag{12}$$

where $\underline{r}_i$ is the radius vector to vertex i, ordered in counterclockwise order around cell point j (Fig. 3a), and $\underline{Z}$ is the unit vector perpendicular to the two dimensional plane. We note that this is equal to $1/3 \sum_k V_k$ where V_k are the triangle volumes. The pressure force term may be expressed as

$$V_j \langle \nabla p_j \rangle = \frac{1}{6} \underline{Z} \times \sum_i p_i (\underline{r}_{i-1} - \underline{r}_{i+1}) \tag{13}$$

for the case where the pressures are defined at cell points. We note that this is equivalent to a volume weighted average of triangle pressure gradients, and therefore this term is consistent with the differential formulation. If the pressure is defined on the triangles, then using the cell of Fig. 3b

$$V_j \langle \underline{\nabla} p_j \rangle = \frac{1}{2} \underline{z} \times \sum_k p_k (\underline{r}_{i-1} - \underline{r}_i). \tag{14}$$

If the triangle pressure is obtained at the centroid by linear interpolation of the vertex pressures:

$$p_k = \frac{1}{3}(p_i + p_j + p_{i-1}), \tag{15}$$

then Eqs. (13) and (14) give precisely the same result.

As is apparent from the above, there is a certain freedom in the choice of pressures at cell points, as suggested following Eq. (11). Another choice is to define the pressure on the triangles, associated with assigning mass to the triangles. Such a choice is natural if multimaterial problems are considered, in which case the triangle sides form interfaces. In this case $p_k = p(\rho_k)$.

There are distinct differences in the numerical methods that emerge based on these choices. In the case of vertex pressures, it is seen that the cell volume, Eq. (12), and hence the cell pressure is independent of the position of the cell point. This implies that certain modes of motion become possible, typically with a high spatial wavenumber, which are not "seen" by the difference equations, and which can arise as a result of boundary conditions, for example. The growth of such a mode can destroy the numerical solution. This behavior typically arises when velocity and pressure are located at the same point[24,25] and the problem is frequently "solved" by filtering, or by the use of viscous "node couplers". The use of triangle pressures eliminates these coupling problems, but it is not without its own difficulties. In the limit of incompressible flow, the use of triangle pressures implies the constancy of triangle volumes. As Fritts and Boris[8] point out, it is not possible to achieve this for most boundary conditions, in a confined volume. While in compressible flow this geometrical restriction is less severe, it can produce strong velocity fluctuations of strictly numerical origin. We have used a linear combination of these two

methods and this frequently works well. There are many other possibilities for getting around these problems and they must be investigated in the future.

The cells we have described are Lagrangian only while neighbors do not change. When neighbors do change, cell volumes change, and therefore cell masses, momenta and energy must change. This requires a local reapportioning of mass, momentum, and energy in a conservative fashion. This is particularly straightforward using the cell of Fig. 3a, since a quadrilateral whose diagonal changes as a result of a neighbor change is shared by all the affected cells. An important point is that following the reapportionment, the mass, momentum, and energy changes are added to the respective cell values, and at present it is not known how to do this reversibly. Thus the process of reapportionment is inherently diffusive and corresponds to a loss of information. Reapportionment may be considered as a form of fluxing that takes place instantaneously, rather than as a continuous process.

Temporal differencing is explicit and follows the practice of PAF[4]:

$$m_j\,(\underline{u}_j^{n+1} - \underline{u}_j^{n}) = -\,\Delta t\; V_j^{n} \langle \underline{\nabla}\, p_j^{n} \rangle$$

$$\underline{x}_j^{n+1} - \underline{x}_j^{n} = \Delta t\; \underline{u}_j^{n+1} \quad . \tag{16}$$

This form of differencing has stability advantages[4] and is time centered for position $\underline{x}$ for constant time steps. The completely time centered scheme is implicit, and although time-reversible and therefore nondiffusive, it does not appear to be worthwhile in view of the nonreversibility of the reapportionment discussed above.

IV. MESH SMOOTHING

We note that in applying Eqs. (4-8) one makes the approximation

$$\phi_j \simeq \frac{1}{V_j} \int_{V_j} \phi dV \ , \tag{17}$$

where ϕ is typically ρ or $\rho \underline{u}$. Expanding ϕ in a Taylor series, we see that

$$\phi_j = \frac{1}{V_j} \int_{V_j} \phi dV - \nabla\phi_j \cdot (\bar{\underline{r}}_j - \underline{r}_j) - \frac{1}{2} \underline{\nabla}\,\underline{\nabla}\phi_j : \overline{(\underline{r} - \underline{r}_j)^2}_j + \cdots$$

where

$$\bar{\underline{r}}_j = \frac{1}{V_j} \int_{V_j} \underline{r} dV \ ,$$

$$\overline{(\underline{r} - \underline{r}_j)^2}_j = \frac{1}{V_j} \int_{V_j} (\underline{r} - \underline{r}_j)^2 \, dV \ . \tag{18}$$

Therefore, our approximation is first order accurate if the cell point is located within the cell, second order accurate if the cell point is at the cell centroid, and the approximation is further improved if the cell is symmetric, so that the product of inertia of the cell area is zero. The construction of the Delaunay mesh ensures that our method is at worst first order. However, in practice the mesh can become very irregular (see examples in Ref. (7)), with cell points far from the cell centroids.

Therefore, to improve accuracy, we introduce a mesh smoothing procedure at each time step following the Lagrangian part of the calculation. The cell centroids are computed at the end of the Lagrangian phase and the cell points are moved some fraction of the distance (typically 0.5) towards them. This defines the mesh velocity $\underline{b}$ in the fluxing terms. Of course, this will not result in the cell point being exactly at the centroid but because of the small time steps required for both accuracy and stability, the cell point will at all times be in the near vicinity of the centroid. The fluxing terms in Eqs. (4,5) are evaluated assuming a linear variation of ρ, $\underline{u}$, and $\underline{b}$ along the cell faces.

It is straightforward to retain a Lagrangian mesh wherever it is nexessary, such as at interfaces or at free surfaces. Frequently, there are large parts of the flow where the mesh does not get distorted in the Lagrangian calculation and it is possible, as well as desirable, to avoid mesh smoothing in these regions. As one result of the mesh smoothing, there is far less neighbor switching since the mesh tends to approach a hexagonal configuration, so that there is, in effect, a trade off between the fluxing due to reapportionment and the fluxing due to smoothing. At no time is the fluxing as severe as in Eulerian calculations since, on the average, the mesh still travels with the flow.

V. COMPUTATIONAL EXAMPLE

As an illustration of the technique described, at its current state of development, a computation of the symmetric, normal impact of two Chaplygin jets was carried out. This is an attractive test problem because it involves a free surface, and because certain analytical results are available [26] for comparison with the calculation.

Two 2-dimensional jets of uniform width (h = 0.01 m), uniform density ($\rho_\infty = 8.9 \times 10^3$ kg/m^3), are assumed to undergo normal inpact. The jets are composed of a single material satisfying the Chaplygin equation of state (see definition following Eq. 3. $k^2 = 1.218 \times 10^6$ GPa kg/m^3). The jets travel at 1.96×10 m/s, which corresponds to a Mach number $M_\infty = 0.5$ at the unperturbed conditions.

The computation was performed using triangle pressures only, mesh smoothing was performed in the region where $|\Delta\rho|/\rho_\infty > 0.01$, and the time step was controlled in the Lagrangian phase by limiting the rate of change of the perimeter of triangles.

Figures 4 and 5 illustrate the early development of the free surface. A high density zone is formed above the plane of contact, and it dissipates as it propagates away from this plane as the steady state is approached. Figure 6 shows the mesh, and Figure 7 shows the density contours and velocity vectors at 25 μs following impact, the termination of the calculation. Figure 6 shows a number of points plotted along the exact free surface at steady state, for comparison. The agreement is reasonable and might be improved by continuing the computation further. The steady state free surface shape is given by the equation

$$Y = \ln[(e^X + 1)/(e^X - 1)] \quad , \tag{19}$$

where

$$X = \frac{\pi}{2h\sqrt{1 - M_\infty^2}} (2x - h) \quad ,$$

and

$$Y = \frac{\pi}{2h\sqrt{1 - M_\infty^2}} (2y - h) \quad .$$

Figures 8 and 9 show the comparison of the calculation with the exact distributions of density and velocity along the x-axis, the plane of contact. The density and velocity distribution along this axis are given by the transcendental equation

$$x = h\left\{1 - \frac{2}{\pi} \tan^{-1} Q + \frac{\sqrt{1 - M_\infty^2}}{\pi} \ln [(Q+1)/(Q-1)]\right\}$$

$$u = k^2 M/\rho_\infty^2 \quad , \tag{20}$$

$$\rho = \rho_\infty/\sqrt{1 - M_\infty^2 + M^2} \quad ,$$

where

$$M = 2\sqrt{1 - M_\infty^2}\, QC/(Q^2C^2 - 1) \quad ,$$

and

$$C = (1 + \sqrt{1 - M_\infty^2})/M_\infty \quad .$$

The agreement with the exact distributions is reasonable, except for the density at the stagnation point. This discrepancy may be due to the calculation not having reached the steady state.

In conclusion, this paper describes a new and promising technique for Lagrangian numerical fluid dynamics. However, much more research remains to be done to investigate variations in the scheme and their effect on the accuracy and performance of the technique.

REFERENCES

1. F. H. Harlow, Proc. Symp. Appl. Math., 15, 269 (1963).

2. D. Greenspan, Comp. Meth. Appl. Mech. Engrg., 3, 293 (1974).

3. R. B. Larson, J. Comput. Phys., 27, 397 (1978).

4. B. J. Daly, F. H. Harlow, and J. E. Welch, "Numerical Fluid Dynamics Using the Particle-and-Force Method", Los Alamos Scientific Laboratory report LA-3144 (1965).

5. F. H. Harlow, "Theory of Correspondence Between Fluid Dynamics and Particle-and-Force Models", Los Alamos Scientific Laboratory report LA-2806 (1963).

6. C. W. Hirt, A. A. Amsden, and J. L. Cook, J. Comput. Phys., 14, 227 (1974).

7. W. P. Crowley, "Proceedings of the Second International Conference on Numerical Methods in Fluid Dynamics", Springer-Verlag, New York/Berlin, (1971).

8. M. J. Fritts and J. P. Boris, J. Comput. Phys., 31, 173 (1979).

9. B. Quentrec and C. Brot, J. Comput. Phys., 13, 430 (1973).

10. C. A. Rogers, "Packing and Covering", Cambridge Univ. Press, London/New York (1964).

11. G. Voronoi, J. Reine Angew. Math., 134, 198 (1908).

12. J. M. Ziman, "Principles of the Theory of Solids", 2nd. Ed., Cambridge Univ. Press, London/New York (1972).

13. J. M. Ziman, "Models of Disorder", Cambridge Univ. Press, London/New York (1979).

14. T. Kiang, Z. Astrophys., 64, 433 (1966).

15. Y. Talmon and S. Prager, J. Chem. Phys., 69, 2984 (1978).

16. P. Pathak, P. H. Winterfeld, H. T. Davis, and L. E. Scriven, Society of Petroleum Engineers paper SPE 8846, presented at the First Joint SPE/DOE Symposium on Enhanced Oil Recovery, Tulsa, OK (1980).

17. M. I. Shamos and D. Hoey, Proc. 16th. Ann. IEEE Symposium on Foundations of Algorithms, Berkeley, CA (1975).

18. B. Dalaunay, Bull. Acad. Sci. USSR (VII), Classe Sci. Mat. Nat., 793 (1934).

19. W. Bristow, J-P. Dussault, and B. L. Fox, J. Comput. Phys., 29, 81 (1978).

20. J. L. Finney, J. Comput. Phys., 32, 137 (1979).

21. P. A. Thompson, "Compressible-Fluid Dynamics", McGraw-Hill, New York (1972).

22. A. T. Peaslee, R. C. Kirkpatrick, H. Trease, Los Alamos, Private communication.

23. A. M. Winslow, J. Comput. Phys., 2, 149 (1967).

24. R. L. Sani, P. M. Gresho, and R. L. Lee, Proc. Third International Conf. on Finite Elements in Flow Problems, Banff, Canada (1980).

25. R. K-C. Chan, J. Comput. Phys., 17, 311 (1975).

26. R. R. Karpp, "An Exact Partial Solution to the Steady-State, Compressible Fluid Flow Problems of Jet Formation and Jet Penetration", Los Alamos Scientific Laboratory report LA-8371 (1980).

FIGURE CAPTIONS

Fig. 1. A fragment of a Voronoi mesh and the associated Delaunay triangulation.

Fig. 2. The continuous transition of the Voronoi mesh as points 1 and 3 move closer together and are connected as neighbors, while points 2 and 4 are disconnected.

Fig. 3. Two alternative definitions of computational cells associated with the cell point j.

Fig. 4. The mesh and the density contours, illustrating the early development of the free surface, at t = 2.65 μs.

Fig. 5. The mesh and the density contours at t = 6.77 μs.

Fig. 6. The mesh at t = 25 μs, and the shape of the free surface from the exact solution at steady state.

Fig. 7. The density contours and velocity vectors at t = 25 μs.

Fig. 8. The exact steady state and the computed (t = 25 μs) density profile along the plane of impact.

Fig. 9. The exact steady state and the computed (t = 25 μs) velocity profile along the plane of impact.

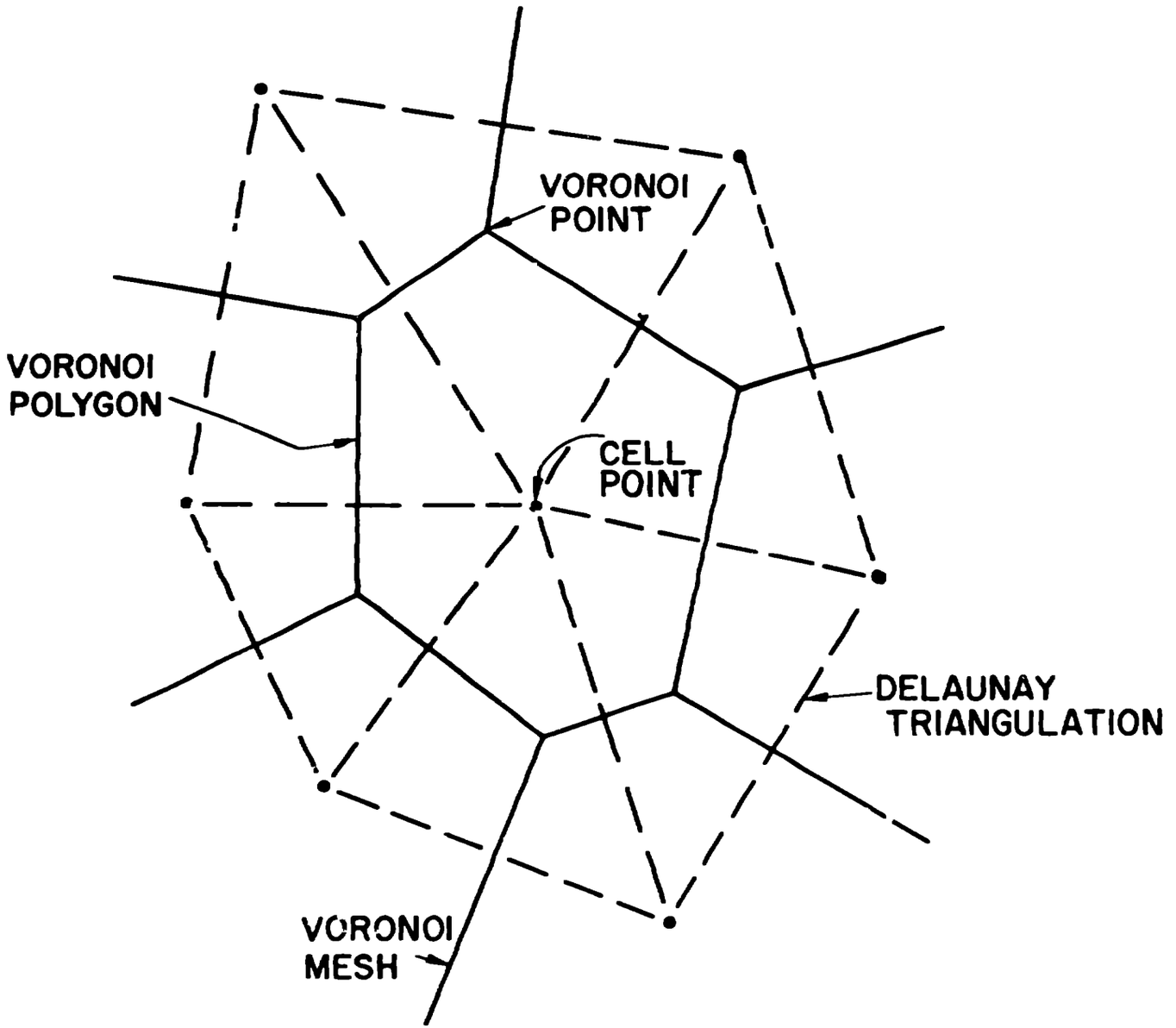
VORONOI
POINT
VORONOI
POLYGON
CELL
POINT
DELAUNAY
TRIANGULATION
VORONOI
MESH

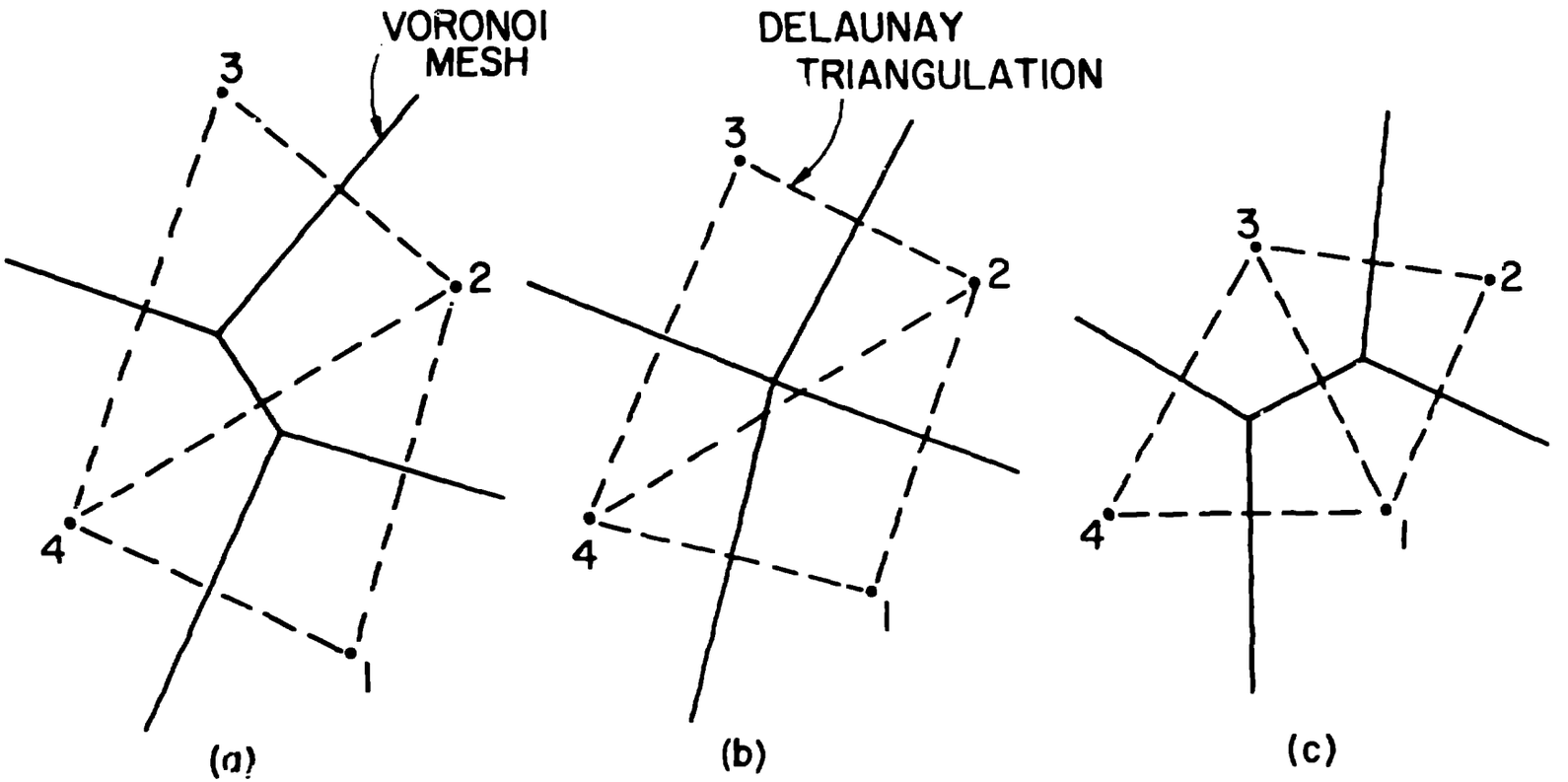
VORONOI
MESH
DELAUNAY
TRIANGULATION
3
2
4
1
(a)
(b)
(c)

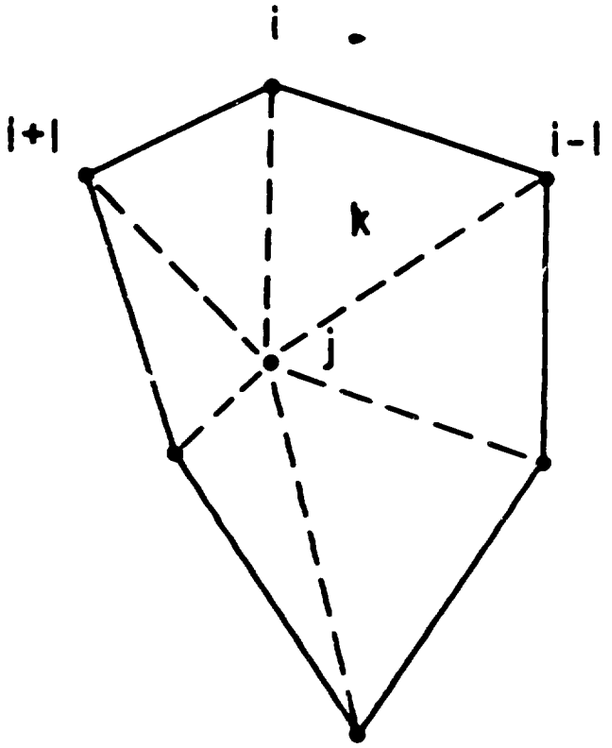

(a)

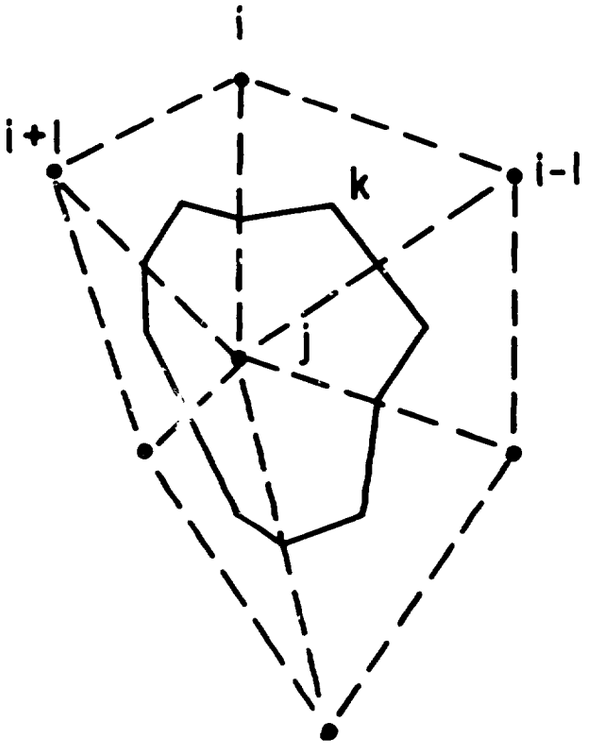

(b)

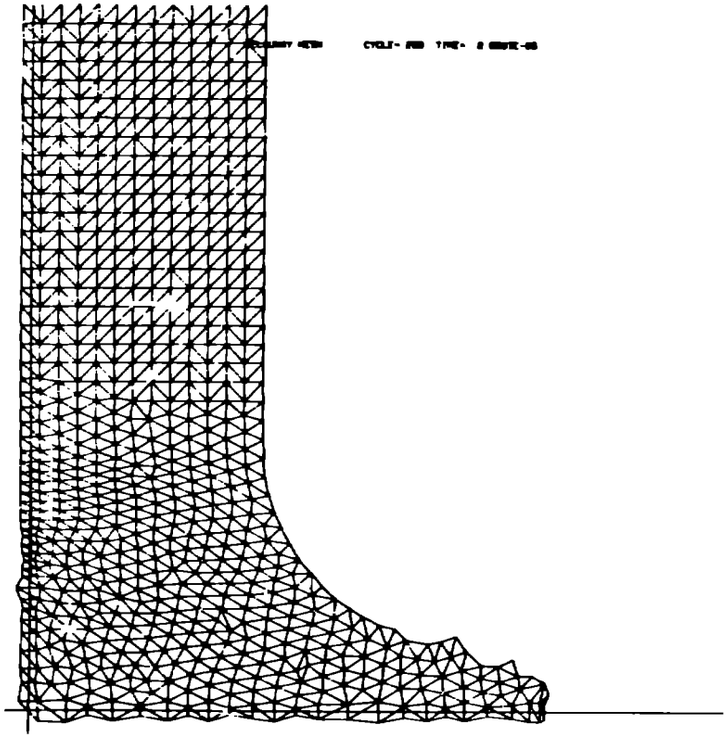

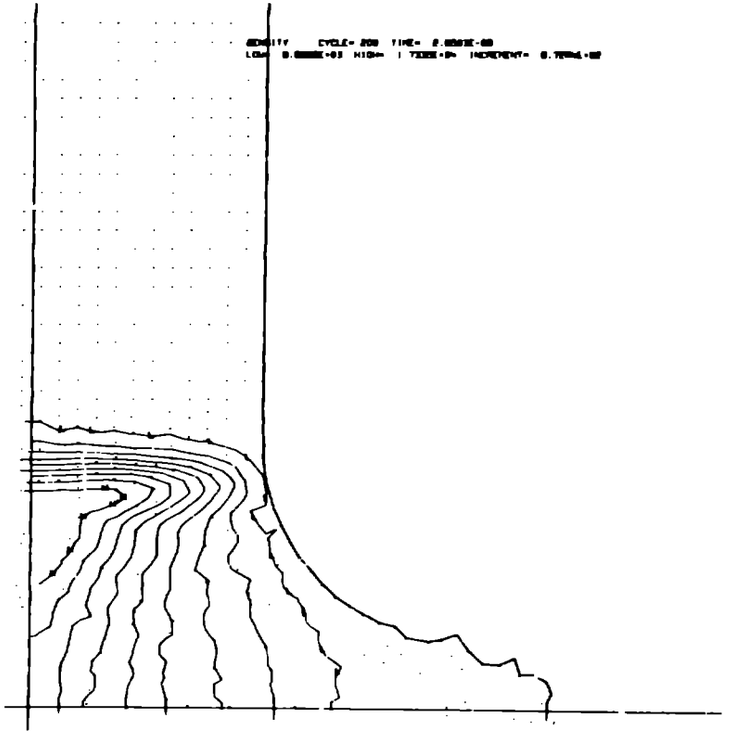

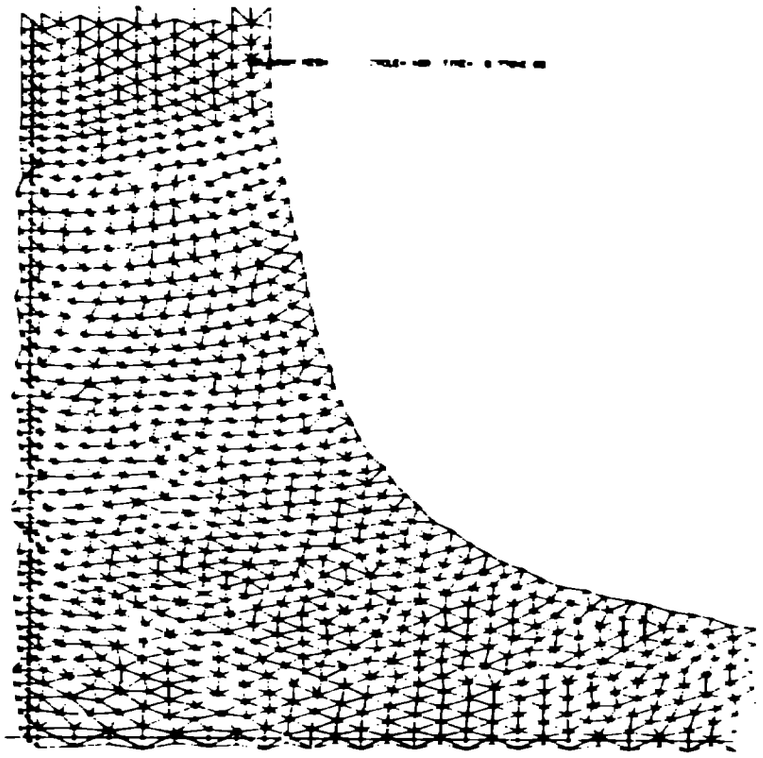

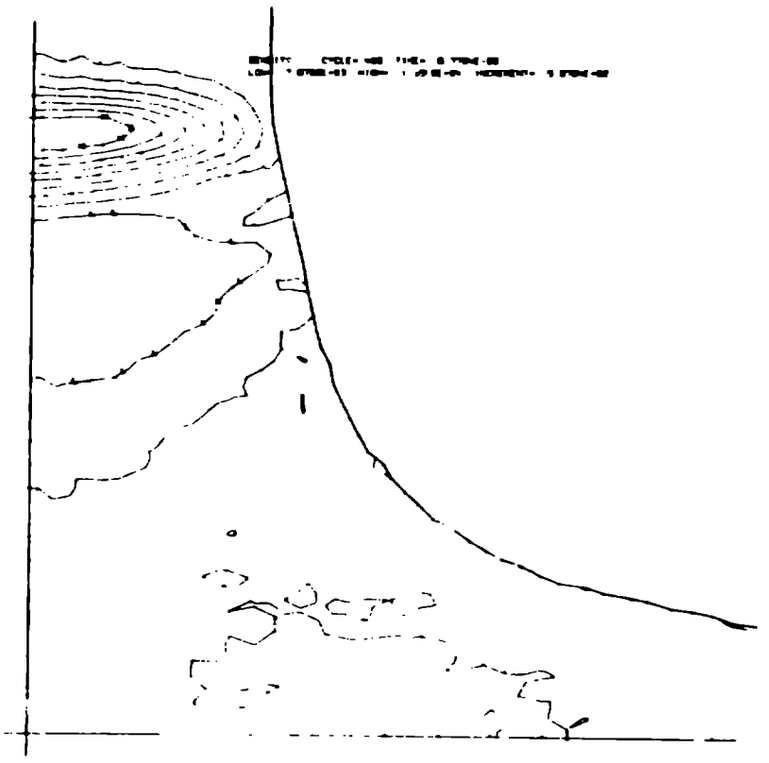

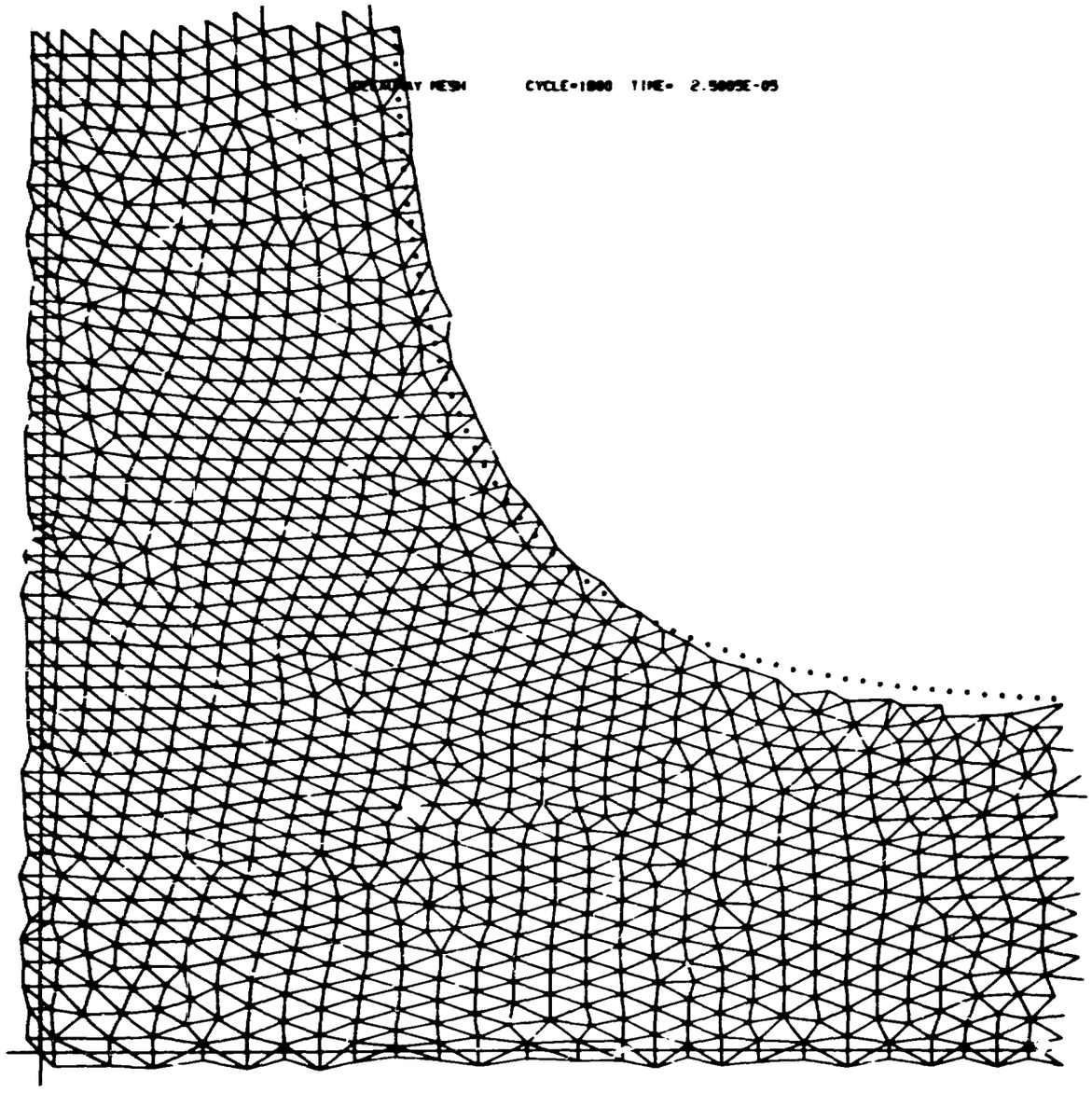
CYCLE=1000 TIME= 2.500E-05

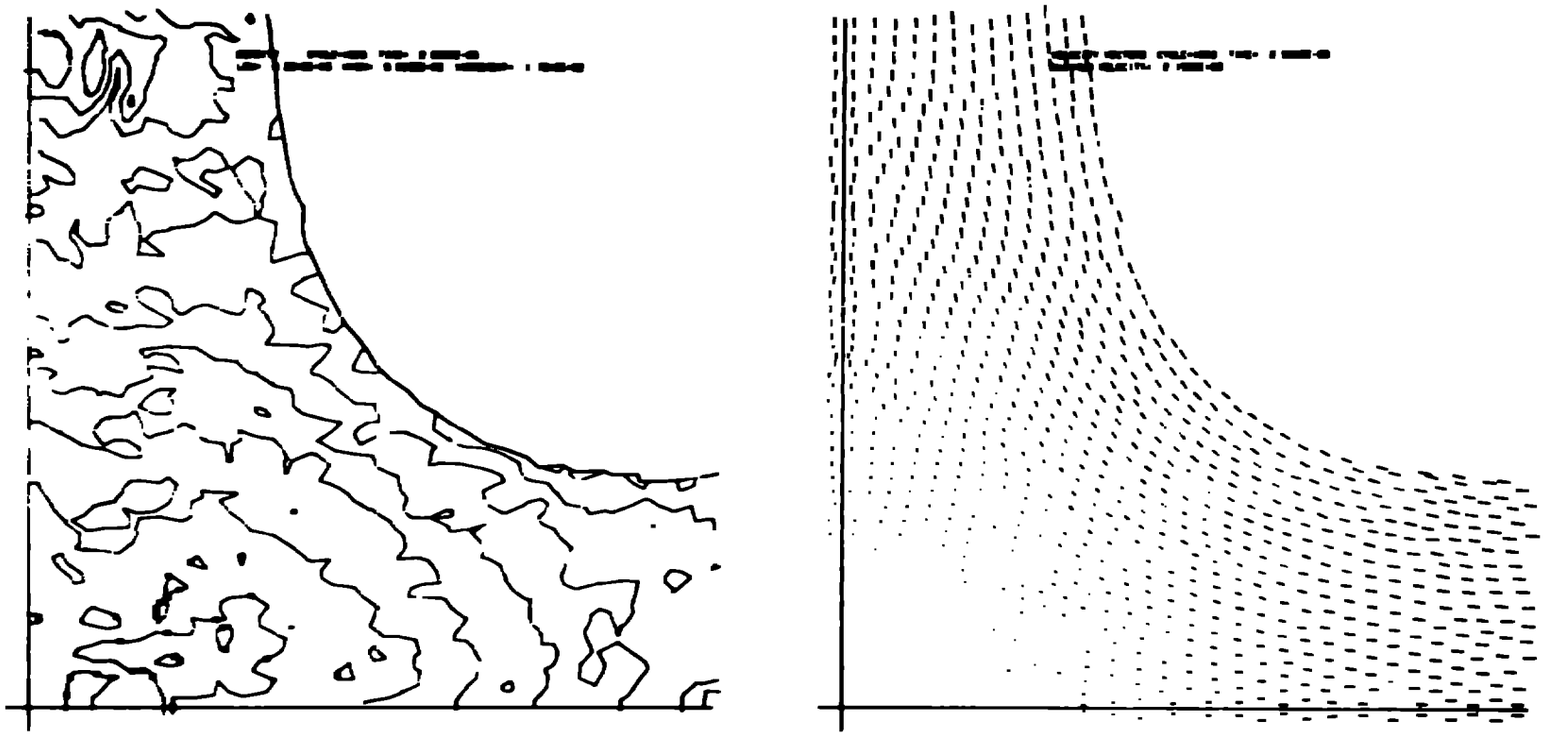

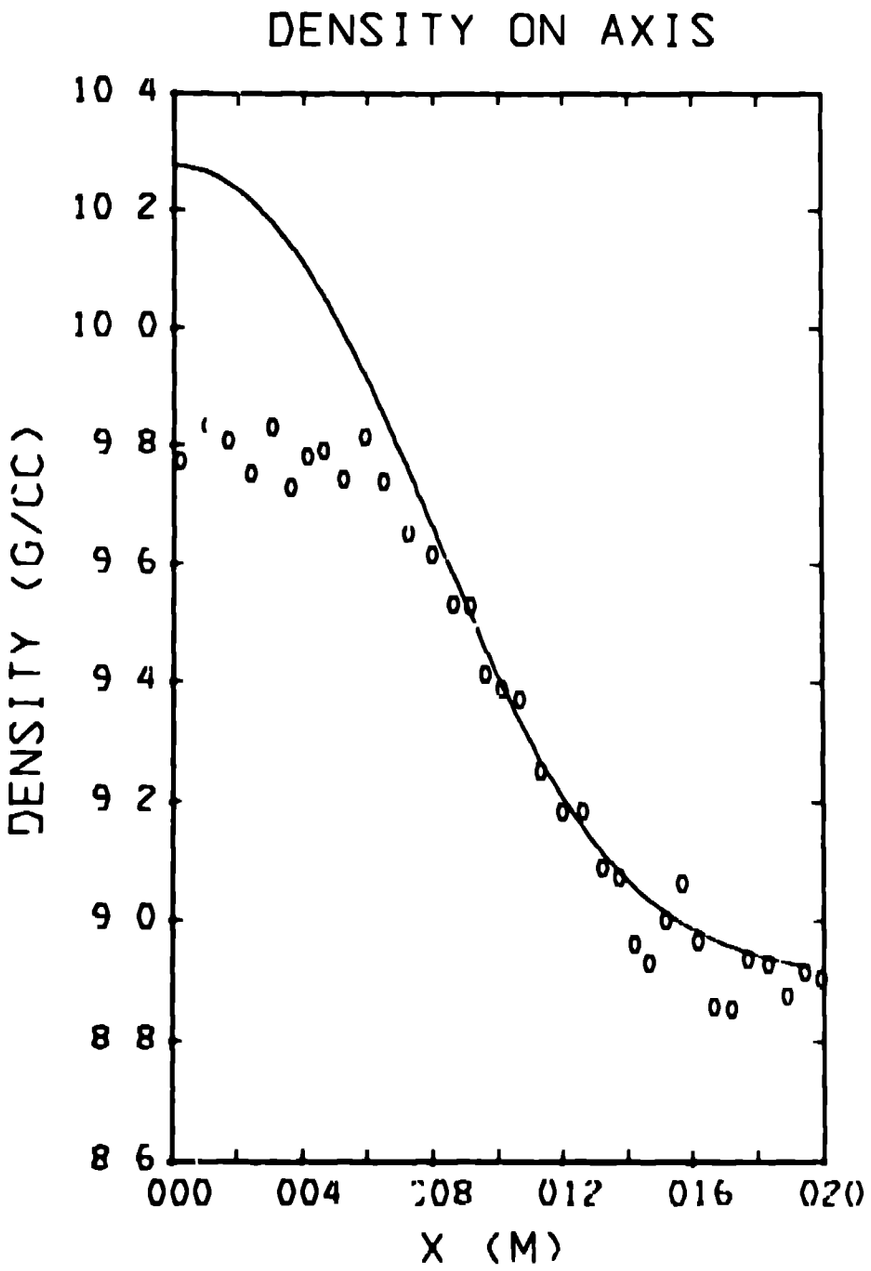
DENSITY ON AXIS
10 4
10 2
10 0
9 8
9 6
9 4
9 2
9 0
8 8
8 6
DENSITY (G/CC)
000
004
008
012
016
020
X (M)

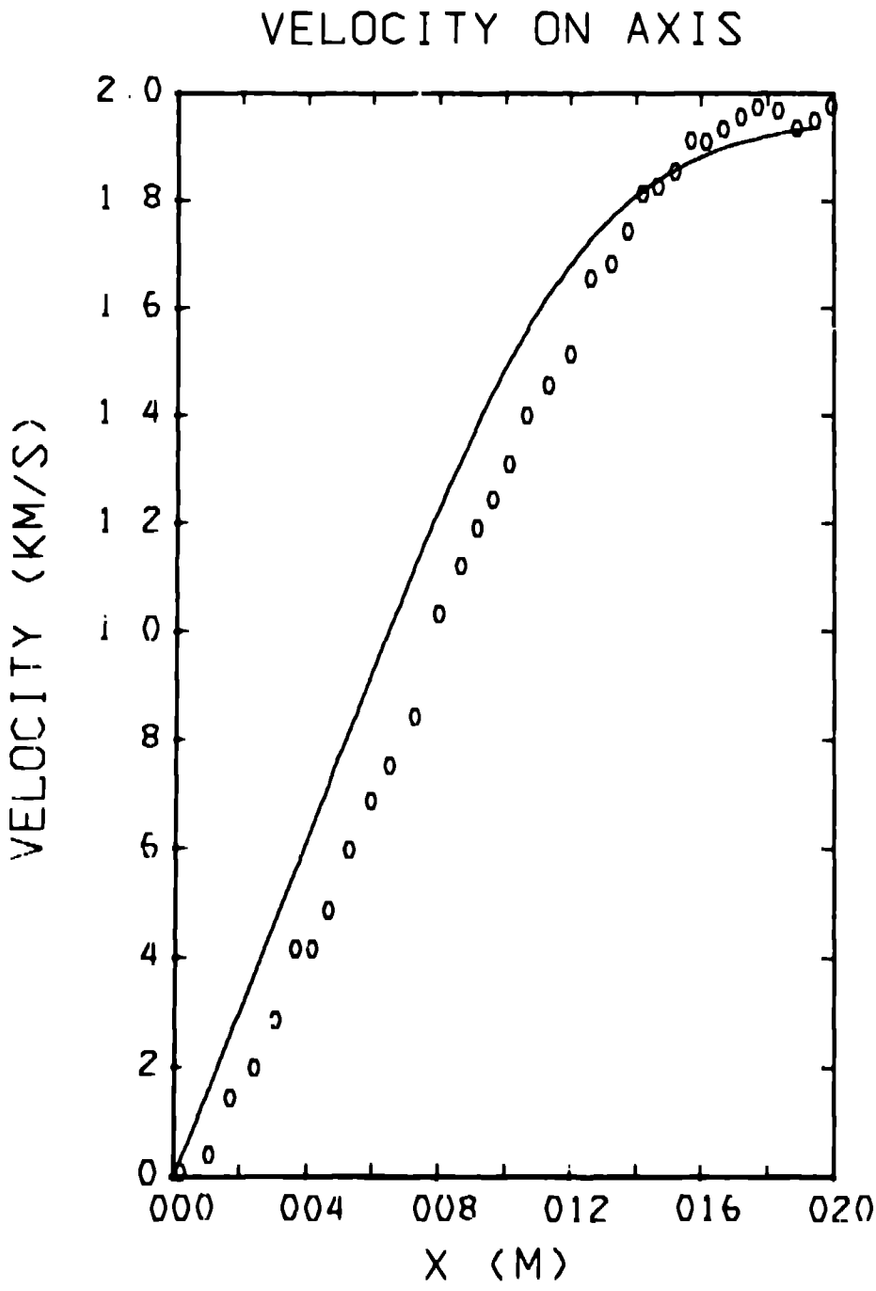
VELOCITY ON AXIS
VELOCITY (KM/S)
2.0
1.8
1.6
1.4
1.2
1.0
.8
.6
.4
.2
0
000
004
008
012
016
020
X (M)